

Flavor ratios of extragalactic neutrinos and neutrino shortcuts in extra dimensions

Elke Aeikens,^a Heinrich Päs,^a Sandip Pakvasa,^b Philipp Sicking^a

^aFakultät für Physik, Technische Universität Dortmund, 44221 Dortmund, Germany

^bDepartment of Physics & Astronomy, University of Hawaii, Honolulu, HI 96822, USA

E-mail: elke.aeikens@tu-dortmund.de, heinrich.paes@tu-dortmund.de,
pakvasa@phys.hawaii.edu, philipp.sicking@tu-dortmund.de

Abstract. The recent measurement of high energy extragalactic neutrinos by the IceCube Collaboration has opened a new window to probe non-standard neutrino properties. Among other effects, sterile neutrino altered dispersion relations (ADRs) due to shortcuts in an extra dimension can significantly affect astrophysical flavor ratios. We discuss two limiting cases of this effect, first active-sterile neutrino oscillations with a constant ADR potential and second an MSW-like resonant conversion arising from geodesics oscillating around the brane in an asymmetrically warped extra dimension. We demonstrate that the second case has the potential to suppress significantly the flux of specific flavors such as ν_μ or ν_τ at high energies.

Keywords: extra dimensions, ultra high energy photons and neutrinos, neutrino theory, neutrino properties

ArXiv ePrint: [1410.0408](https://arxiv.org/abs/1410.0408)

Contents

1	Introduction	1
2	ADR due to sterile neutrino shortcuts	1
3	Constant ADR potential	2
4	MSW-like resonant conversion	5
5	Conclusion	10

1 Introduction

Recently the IceCube Collaboration has reported the detection of 37 neutrino events in the energy range of 30 TeV up to 2 PeV. Atmospheric neutrinos as the source of this signal are ruled out at more than 5.7 sigma [1] and it has been argued that these neutrinos are extragalactic in origin [2]. Consequently this result allows for the first time to study the flavor composition of high energy extra-galactic neutrinos and thus opens up a window onto neutrino properties exhibiting themselves at extreme energies and propagation distances. An apparent deficit of muon track events in the IceCube data has been discussed as a possible indication for new physics beyond the Standard Model [3–5], albeit this anomaly is so far not statistically significant [6]. In spite of the seeming deficit of muons, several flavor analyses of IceCube events find that the data are consistent with the expected canonical mix of 1:1:1 [7–10]. On the other hand a recent spectral analysis [8] points towards an energy dependent flavor composition with muon and tau neutrino depletion at high energies while the analysis [10] prefers a best fit flavor ratio of 0:0.2:0.8, both of which are very hard to understand without invoking new physics. However, more statistics is needed to determine the flavor ratio of extra-galactic neutrinos and a deviation from 1:1:1 to probe any signatures of such new physics.

2 ADR due to sterile neutrino shortcuts

In this paper we discuss how scenarios in which the simple dispersion relation $E^2 = p^2 + m^2$ is altered due to sterile neutrino shortcuts in extra dimensions [11] can affect these flavor ratios. For example, sterile neutrinos propagating in spacetimes with an asymmetrically warped extra dimension u [12–14]

$$ds^2 = dt^2 - \sum_{i=1}^3 \eta^2(u) (dx^i)^2 - du^2 \quad (2.1)$$

propagate on geodesics oscillating around the brane [15] and experience a shorter propagation time [11] which can be parametrized by a shortcut parameter defined as the normalized difference of propagation times on the brane and in the bulk, $\epsilon \equiv \delta t/t$. While being speculative, such scenarios where sterile neutrinos acquire altered dispersion relations are motivated by several anomalies in neutrino oscillations experiments and cosmology, for an overview see [16].

As a consequence, the effective neutrino masses and mixing are altered in a way similar to what happens when neutrinos propagate inside matter [11], so that the effective two-flavor oscillation amplitude becomes

$$\sin^2 2\tilde{\theta} = \frac{\sin^2 2\theta}{\sin^2 2\theta + \cos^2 2\theta \left[1 - \left(\frac{E}{E_{\text{Res}}} \right)^2 \right]^2}, \quad (2.2)$$

and the Hamiltonian is altered by the additional term

$$\delta\tilde{H} = \frac{\delta m^2}{2E} \sqrt{\sin^2 2\theta + \cos^2 2\theta \left(1 - \left(\frac{E}{E_{\text{Res}}} \right)^2 \right)}, \quad (2.3)$$

where E_{Res} denotes the resonance energy

$$E_{\text{Res}} = \sqrt{\frac{\delta m^2 \cos 2\theta}{2\epsilon}}. \quad (2.4)$$

Note that for energies much smaller than the resonance energy E_{Res} , the change in the dispersion relation due to the extra-dimensional shortcut decouples and the scenario discussed resembles the standard scenario with three active and one sterile neutrino.

Further details of such models have been worked out in [17–20] and a similar effect due to the interaction with the matter potential of intergalactic dark matter has been discussed in [21].

3 Constant ADR potential

Astrophysical neutrinos are typically assumed to originate from a pion source where the dominant number of neutrinos is produced in the decays of charged pions and kaons resulting from high energy proton-proton and few proton-photon collisions [22, 23], $p + p \rightarrow \pi^\pm \rightarrow \mu^\pm + \nu_\mu^{(-)} \rightarrow e^\pm + \nu_e^{(-)} + \nu_\mu + \bar{\nu}_\mu$. In this case the initial flavor ratio at the source is

$$(\Phi_e^0 : \Phi_\mu^0 : \Phi_\tau^0) = (1 : 2 : 0), \quad (3.1)$$

where Φ_α denotes the integrated flux of both neutrinos and anti-neutrinos. To estimate the flavor ratios after propagation from the source to the detector we follow [24].

As neutrino oscillations decohere over the large propagation distances the flavor conversion is properly described by the mean of the oscillation probability so that the oscillatory term averages out to $\sin^2(x/L_{\text{osz}}) \sim 1/2$ and the conversion probability $P_{\alpha\beta}$ and consequently the normalized neutrino fluxes depend only on the mixing matrix elements,

$$\Phi_\alpha = \sum_\beta P_{\alpha\beta} \Phi_\beta^0, \quad P_{\alpha\beta} = \sum_i |U_{\alpha i}|^2 |U_{\beta i}|^2. \quad (3.2)$$

Adopting a 3+1 scenario, $U_{\alpha i}$ denotes a 4×4 mixing matrix including a sterile neutrino mixing with ν_μ and ν_τ . The flavor ratios at the detection point are then given by $(\Phi_{\nu_e} : \Phi_{\nu_\mu} : \Phi_{\nu_\tau} : \Phi_{\nu_s})$, with the neutrino fluxes Φ_β and $\beta \in \{\nu_e, \nu_\mu, \nu_\tau, \nu_s\}$.

For the 3×3 sub matrix we adopt an approximate tribimaximal mixing scheme according to [25]

$$U_{TBM} = \frac{1}{\sqrt{6}} \begin{pmatrix} 2 & \sqrt{2} & 0 \\ -1 & \sqrt{2} & \sqrt{3} \\ -1 & \sqrt{2} & -\sqrt{3} \end{pmatrix} \Rightarrow P_{TBM} = \frac{1}{18} \begin{pmatrix} 10 & 4 & 4 \\ 4 & 7 & 7 \\ 4 & 7 & 7 \end{pmatrix}. \quad (3.3)$$

which, following [26], is complemented by the matrices O^{e4} , $O^{\mu4}$, $O^{\tau4}$ modeling the admixture of the sterile neutrino. The rotation matrices $O^{\alpha4}$ are defined as

$$O^{e4} = \begin{pmatrix} c_e & 0 & 0 & s_e \\ 0 & 1 & 0 & 0 \\ 0 & 0 & 1 & 0 \\ -s_e & 0 & 0 & c_e \end{pmatrix}, \quad O^{\mu4} = \begin{pmatrix} 1 & 0 & 0 & 0 \\ 0 & c_\mu & 0 & s_\mu \\ 0 & 0 & 1 & 0 \\ 0 & -s_\mu & 0 & c_\mu \end{pmatrix}, \quad O^{\tau4} = \begin{pmatrix} 1 & 0 & 0 & 0 \\ 0 & 1 & 0 & 0 \\ 0 & 0 & c_\tau & s_\tau \\ 0 & 0 & -s_\tau & c_\tau \end{pmatrix}, \quad (3.4)$$

with the abbreviations $s_\alpha = \sin \theta_\alpha$ and $c_\alpha = \cos \theta_\alpha$. This yields the 4×4 mixing matrix $U = U_{TBM} O^{e4} O^{\mu4} O^{\tau4}$,

$$U = \frac{1}{\sqrt{6}} \begin{pmatrix} 2c_e & \sqrt{2}c_\mu - 2s_e s_\mu & -s_\tau (2c_\mu s_e + \sqrt{2}s_\mu) & c_\tau (2c_\mu s_e + \sqrt{2}s_\mu) \\ -c_e & \sqrt{2}c_\mu + s_e s_\mu & s_\tau (c_\mu s_e - \sqrt{2}s_\mu) + \sqrt{3}c_\tau & -c_\tau (c_\mu s_e - \sqrt{2}s_\mu) + \sqrt{3}s_\tau \\ -c_e & \sqrt{2}c_\mu + s_e s_\mu & s_\tau (c_\mu s_e - \sqrt{2}s_\mu) - \sqrt{3}c_\tau & -c_\tau (c_\mu s_e - \sqrt{2}s_\mu) - \sqrt{3}s_\tau \\ -\sqrt{6}s_e & -\sqrt{6}c_e s_\mu & -\sqrt{6}c_e c_\mu s_\tau & \sqrt{6}c_e c_\mu c_\tau \end{pmatrix}, \quad (3.5)$$

For sake of simplicity we assume either only one mixing angle with the additional state to be non-zero ($s_\alpha \equiv \sin \theta$ and $s_\beta|_{\beta \neq \alpha} = 0$) or two mixing angles being the same, for instance $s_\mu = s_\tau \equiv \sin \theta$ and $s_e = 0$. This allows to calculate the normalized neutrino fluxes resulting from an initial $(\Phi_e^0 : \Phi_\mu^0 : \Phi_\tau^0 : \Phi_s^0) = (1 : 2 : 0 : 0)$ flavor ratio as follows,

$$\Phi_e = \frac{1}{3} \Phi_{tot} (P_{ee} + 2P_{e\mu}), \quad (3.6)$$

$$\Phi_\mu = \frac{1}{3} \Phi_{tot} (P_{e\mu} + 2P_{\mu\mu}), \quad (3.7)$$

$$\Phi_\tau = \frac{1}{3} \Phi_{tot} (P_{e\tau} + 2P_{\tau\mu}), \quad (3.8)$$

$$\Phi_s = \frac{1}{3} \Phi_{tot} (P_{es} + 2P_{s\mu}). \quad (3.9)$$

As a consequence, an initial pion source spectrum of 1:2:0 is transformed into the expected flavor ratio of 1:1:1 at the point of detection (see e.g. [27–29]).

In order to illustrate the effect of neutrino shortcuts we concentrate on two concrete scenarios for sterile neutrinos:

- A scenario with light sterile neutrinos motivated by the LSND, MiniBoone and Gallium anomalies with a δm^2 of order 1 eV². Here we use $\sin^2(2\theta) \simeq 0.12$ ($\sin^2 \theta \simeq 0.03$) and $\delta m^2 \simeq 1$ eV². The parameters used here are compatible with the constraints of $|U_{\mu 4}|^2 \lesssim 0.03$ and $|U_{\tau 4}|^2 \lesssim 0.3$ at 90% CL presented in [16]. Note that to explain the LSND and MiniBoone anomalies, a non-zero U_{e4} mixing is necessary. Here we consider these values for various mixing schemes for illustrative purposes and in particular for the case of $(\nu_\mu, \nu_\tau) - \nu_4$ -mixing. For the case of $(\nu_e, \nu_\mu) - \nu_4$ mixing, compare Table 1.

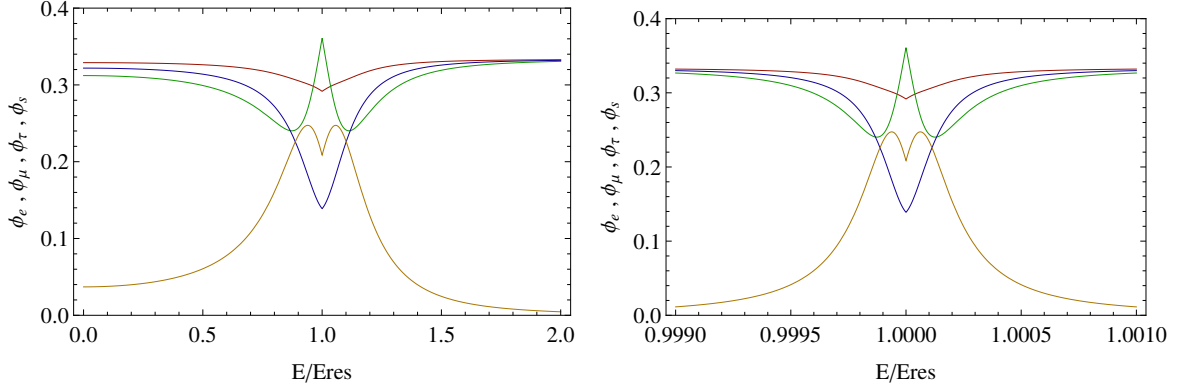


Figure 1. Neutrino flavor rates for a pion source as a function of E/E_{Res} : Φ_e (red), Φ_μ (green), Φ_τ (blue), Φ_s (yellow). Left panel: light sterile neutrino with $\sin^2(2\theta) = 0.12$, $\delta m^2 = 1 \text{ eV}^2$. Right panel: νMSM neutrino with $\sin^2(2\theta) = 10^{-7}$, $\delta m^2 = 1 \text{ keV}^2$.

- The neutrino Minimal Standard Model (νMSM) where a keV scale warm dark matter neutrino is introduced. Here we use $\delta m^2 \simeq 1 \text{ keV}^2$ and $\sin^2(2\theta) \simeq 10^{-7}$ ($\sin^2 \theta \simeq 10^{-8}$). [30].

For an estimation how large the portion of the neutrino spectrum affected by the resonance is it is helpful to calculate the Full Width in energy at a fraction f of Maximum (FWfM) [11] as

$$\frac{\delta E(\text{FWfM})}{E_{\text{Res}}} = \left[1 + \tan 2\theta \sqrt{\frac{1-f}{f}} \right]^{1/2} - \left[1 - \tan 2\theta \sqrt{\frac{1-f}{f}} \right]^{1/2}, \quad (3.10)$$

which, for small θ reduces to $2\theta \sqrt{\frac{1-f}{f}}$. Thus, the resonance is very narrow for a small mixing angle. For example, Full Width at Half Max is $\delta E(\text{FWHM}) = 2\theta E_{\text{Res}}$ for a small angle. Assuming a resonance energy of 300 TeV yields $\delta E(\text{FWHM}) = 104 \text{ TeV}$ (35%), 95 MeV ($3 \cdot 10^{-2}\%$) for the light sterile and νMSM scenarios above, respectively. This demonstrates that the affected portion of the neutrino spectrum depends crucially on the active-sterile neutrino mixing.

In figure 1 the resonance peaks are shown as a function of E/E_{Res} in the light sterile neutrino (left panel) and νMSM scenario (right panel).

In case of the νMSM scenario, an energy resolution up to the order of $10^{-2}\%$ is needed to see a substantial modification in the spectrum which is not accessible for current experiments also in view of limited statistics. In the case of the light sterile neutrino scenario and a resonance energy in the 100 TeV region a significant portion of the neutrino spectrum is affected and is expected to be seen with higher statistics in experiments like IceCube.

In Table 1 we summarize the change in flavor ratios at resonance energies in the light sterile neutrino for different astrophysical sources and mixing scenarios in addition to the one presented above, the pion source with $(\nu_\mu, \nu_\tau) - \nu_4$ mixing. The sources are considered to be ideal, based on processes described in [24]. Also given are the flavor ratios $R = \Phi_\mu/(\Phi_e + \Phi_\tau)$, $S = \Phi_e/\Phi_\tau$, $T = \Phi_\mu/\Phi_{\text{tot}}$ and $G = \Phi_{\bar{e}}/\Phi_{\text{tot}}$, with $\Phi_{\text{tot}} = \Phi_{e/\bar{e}} + \Phi_{\mu/\bar{\mu}} + \Phi_{\tau/\bar{\tau}}$.

The breaking of the original $\mu - \tau$ symmetry in the fluxes obtained results from the additional mixing of both flavors with the sterile neutrino. A similar effect due to a non-vanishing

$\sin \theta_{13} \neq 0$ has been found in [31].

source	Φ_β^0	mixing	$\Phi_\beta(\theta^{\alpha 4})$	R	S	T	G
Pion	1:2:0:0	none ($\theta^{\alpha 4} = 0$)	1:1:1:0	1/2	1	1/3	1/9
		$\nu_e - \nu_4$	4:11:11:6	11/19	8/11	11/30	4/45
		$\nu_\mu - \nu_4$	5:5:5:3	1/2	1	1/3	1/9
		$(\nu_e, \nu_\mu) - \nu_4$	32:41:41:30	41/73	32/41	41/114	16/171
		$(\nu_\mu, \nu_\tau) - \nu_4$	21:26:10:15	26/31	21/10	26/57	7/57
Damped Muon	0:1:0:0	none ($\theta^{\alpha 4} = 0$)	4:7:7:0	7/11	4/7	7/18	2/27
		$\nu_e - \nu_4$	4:9:9:2	9/13	4/9	9/22	2/33
		$\nu_\mu - \nu_4$	1:2:2:1	2/3	1/2	2/5	1/15
		$(\nu_e, \nu_\mu) - \nu_4$	16:115:115:42	115/131	16/115	115/246	8/369
		$(\nu_\mu, \nu_\tau) - \nu_4$	7:16:4:9	16/11	7/4	16/27	7/81
Neutron Beam	1:0:0:0	none ($\theta^{\alpha 4} = 0$)	5:2:2:0	2/7	5/2	2/9	5/27
		$\nu_e - \nu_4$	2:1:1:2	1/3	2	1/4	1/2
		$\nu_\mu - \nu_4$	3:1:1:1	1/4	3	1/5	3/5
		$(\nu_e, \nu_\mu) - \nu_4$	10:1:1:6	1/11	10	1/12	5/12
		$(\nu_\mu, \nu_\tau) - \nu_4$	35:14:14:9	2/7	5/2	2/9	5/9

Table 1. Difference in flavor rates with $\nu_\alpha - \nu_4$ mixing. Here Φ_β^0 denotes the ratio of initial neutrino rates at the source, $(\Phi_e^0 : \Phi_\mu^0 : \Phi_\tau^0 : \Phi_s^0)$, $\Phi_\beta(\theta^{\alpha 4} = 0)$ denotes the ratio of neutrino rates assuming zero active-sterile neutrino mixing, $(\Phi_e : \Phi_\mu : \Phi_\tau : \Phi_s)$, and $\Phi_\beta(\theta^{\alpha 4})$ denotes the ratio of neutrino rates with active-sterile neutrino mixing at resonance energies, $E = E_{res}$.

4 MSW-like resonant conversion

A particularly interesting limit exists in the case where the change in the dispersion relation occurs adiabatically so that an MSW-like [32–34] resonant conversion can occur (for details see [35]). A crucial point in this scenario is that the flavors produced at the source do not propagate as mass eigenstates in vacuum but as eigenstates of the Hamiltonian which have a different admixture of the sterile state due to the change in the dispersion relation. Depending on the scenario, a large amount of muon and tau neutrino depletion can be obtained in case of a normal hierarchy if only the heavier mass eigenstates undergo resonant conversion into sterile neutrinos while the lightest eigenstate does not. In case of inverse hierarchy the same can be achieved if only the heaviest and the lightest mass eigenstates undergo the resonant conversion. We thus assume a scenario where we introduce two sterile neutrinos with a small admixture in the mass eigenstates ν_2 and ν_3 . The mass eigenstate ν_1 which has the maximal contribution of electron neutrinos does not mix with the sterile neutrinos. While ν_2 and ν_3 undergo resonant conversion into sterile neutrinos ν_1 thus will be not affected and the only active component surviving and to be measured. Consequently, a total depletion of ν_2 and ν_3 would result in a $U_{e1}^2 : U_{\mu 1}^2 : U_{\tau 1}^2 \simeq 4 : 1 : 1$ flavor ratio above the resonance energy. Moreover, in a scenario where only ν_1 and ν_2 mix with the sterile neutrinos, ν_3 would be the only active component to survive, resulting in a flavor ratio of $U_{e3}^2 : U_{\mu 3}^2 : U_{\tau 3}^2 \simeq 0 : 1 : 1$, again above the resonance energy. In both cases large deviations from the expected $1 : 1 : 1$ flavor ratio can arise.

Current analyses do not exclude the canonical ratio of 1:1:1 but feature different best fits given as $0 : 0.2 : 0.8$ [10] and $0.92 : 0.08 : 0$ [8], depending on the spectral information included in the fit. The altered flavor ratios arising in the extra-dimensional shortcut scenarios discussed in this paper can at least partly and in specific energy ranges account for such a depletion of electron or muon and tau neutrino flux. In particular a flavor ratio of $4 : 1 : 1$ resembles the best fit in [8].

For sake of simplicity, in the following we discuss a 1+1 active-sterile neutrino pattern with a single non-zero mixing angle θ between an active neutrino ν_a and a sterile one ν_s . As long as the shortcut parameter of an asymmetrically warped extra dimension varies adiabatically in this case the neutrino remains in its original eigenstate of the Hamiltonian. If the dispersion relation varies in a way that would generate level crossing in the non-adiabatic regime, the adiabatic limit would lead to resonant conversion. This gives rise to the following probabilities to detect an active or sterile neutrino in an original beam of pure active neutrinos at its source:

$$P_{\nu_a \rightarrow \nu_a}(x) = \cos^2 \theta \cdot \cos^2 \tilde{\theta} + \sin^2 \theta \cdot \sin^2 \tilde{\theta} \quad (4.1)$$

$$P_{\nu_a \rightarrow \nu_s}(x) = \sin^2 \theta \cdot \cos^2 \tilde{\theta} + \cos^2 \theta \cdot \sin^2 \tilde{\theta} \quad (4.2)$$

Here θ denotes the “vacuum” mixing angle (i.e. bare angle without ADR effects), whereas $\tilde{\theta}$ is the effective mixing angle given in equation (2.2) evaluated at the detection point. We adopt the metric (2.1) with $\eta^2(u) = e^{-2k|u|}$. This leads to a geodesic oscillating around the brane given by

$$u(x) = \pm \frac{1}{2k} \ln[1 + k^2 x(l - x)], \quad (\text{with } 0 \leq x < l). \quad (4.3)$$

The shortcut parameter

$$\epsilon = 1 - e^{-k|u|} = 1 - \frac{1}{\sqrt{1 + k^2 x(l - x)}} \quad (4.4)$$

now depends on the travel distance, which leads to the effective mixing angle

$$\cos 2\tilde{\theta} = \frac{\cos 2\theta - \frac{2E^2}{\delta m^2} \left(1 - \frac{1}{\sqrt{1 + k^2 x(l - x)}}\right)}{\sqrt{\left(\frac{2E^2}{\delta m^2} \left(1 - \frac{1}{\sqrt{1 + k^2 x(l - x)}}\right) - \cos 2\theta\right)^2 + \sin^2(2\theta)}}. \quad (4.5)$$

As pointed out in [15], the geodesic (4.3) repeats itself after $x = l$ to the opposite direction of the brane ($u(x + l) = -u(x)$). This results in a periodicity of ϵ and therefore of the effective mixing angle $\tilde{\theta}$ with the periodic length l . It thus is sufficient to use the definition above with $0 \leq x < l$. For larger travel distances we exploit the periodic behavior $\cos 2\tilde{\theta}(x) = \cos 2\tilde{\theta}(x + l)$, see [15, 35] for details. The periodic length l is a function of the initial conditions for the velocities and of the warp factor k [15]:

$$l = 2 \frac{|\dot{u}_0|}{k \dot{x}_0}, \quad (4.6)$$

where \dot{x}_0 and \dot{u}_0 denote the initial speed of the sterile neutrino along and perpendicular to the brane, respectively.

The limit of resonant conversion applies as long as the change in the dispersion relation is adiabatic, corresponding to the following condition:

$$\gamma_{res} = \frac{4E^3}{(\delta m^2)^2 \sin^2(2\theta)} \left. \frac{d\epsilon}{dx} \right|_{res} \ll 1 \quad (4.7)$$

where the shortcut parameter ϵ is given by (4.4). This is the condition for adiabatic transition at resonance. If the condition is fulfilled at resonance, it is fulfilled everywhere else. As the derivative of the shortcut parameter ϵ with respect to the baseline x at resonance becomes rather complicated, for sake of simplicity we adopt the maximum value of $\frac{d\epsilon}{dx}$ at $x = 0$ as an upper bound:

$$\left. \frac{d\epsilon}{dx} \right|_{res} < \left. \frac{d\epsilon}{dx} \right|_{max} = \frac{1}{2} k^2 l. \quad (4.8)$$

Consequently, if the condition

$$\gamma_{max} = \frac{2E^3}{(\delta m^2)^2 \sin^2(2\theta)} k^2 l \ll 1 \quad (4.9)$$

is fulfilled, the adiabatic condition is fulfilled as well.

As can be seen in (4.5) the survival probability depends on the travel distance of the neutrinos. The survival probability is shown in Figure 2 for different values of k and different energies. For larger values of k the probability becomes steeper in the region of $x = 0, l$, but is nearly constant at its minimal value $P_{min} = \frac{1}{2}(1 - \cos(2\theta))$ for all travel distances, which are longer than the resonance length. In the following we distinguish two cases: First, the periodic length is larger than the travel distance. For this case it is crucial that the resonance crossing occurs during the propagation distance, which is satisfied if the resonance length

$$x_{res} = \frac{l}{2} - \sqrt{\frac{l^2}{4} + \frac{1}{k^2} \left(1 - \frac{1}{1 - \frac{\delta m^2 \cos 2\theta}{2E^2}} \right)} \approx \frac{1}{k^2 l} \frac{\delta m^2 \cos 2\theta}{2E^2} \quad (4.10)$$

is much smaller than the diameter of the Milky Way. This leads to

$$x_{res} < 10^6 \text{ly} = 5 \cdot 10^{25} \frac{1}{\text{eV}} \quad (4.11)$$

$$\Rightarrow k^2 l > \frac{1}{5} 10^{-25} \text{eV} \frac{\delta m^2 \cos 2\theta}{2E^2}. \quad (4.12)$$

If this condition is satisfied the survival probability becomes P_{min} , which is nearly negligible due to the small vacuum mixing angle θ . The approximation in equation (4.10) is valid if the second term in the square root is small compared to the first one, which leads to the condition

$$\frac{\delta m^2 \cos 2\theta}{2E^2} + \frac{l^2 k^2}{4} \gg \frac{\delta m^2 \cos 2\theta}{2E^2} \cdot \frac{l^2 k^2}{4}. \quad (4.13)$$

This condition holds in our context since we only consider high energies and therefore $\frac{\delta m^2 \cos 2\theta}{2E^2} \ll 1$.

Second, the periodic length is smaller than the typical travel distance. Due to the assumption that the events measured by IceCube do not have one common origin, the neutrinos arriving

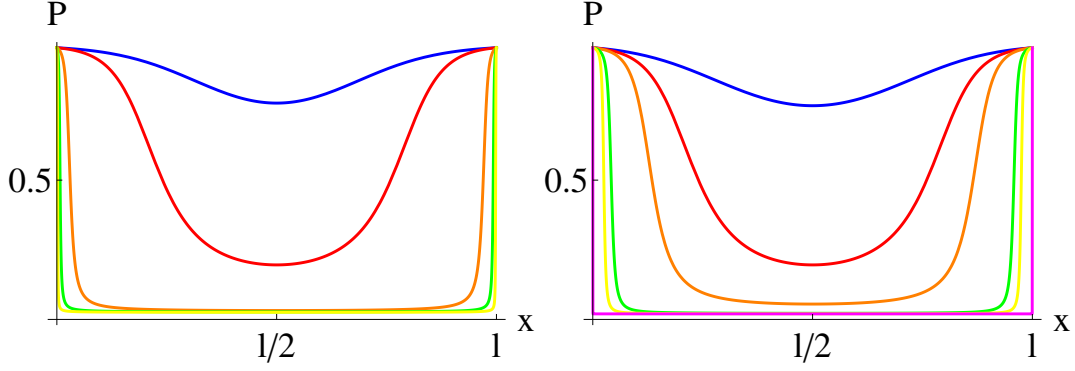


Figure 2. Survival probability (4.1) as a function of the travel distance x for various geometric factors k (left panel, blue: $k = 3/l$, red: $k = 4/l$, orange: $k = 10/l$, green: $k = 20/l$, yellow: $k = 40/l$; adopting $\frac{\delta m^2}{E^2} = 1$ to illustrate the dependence on k) and energies E (right panel, blue: $E^2 = 0.8 \cdot \delta m^2$, red: $E^2 = 1 \cdot \delta m^2$, orange: $E^2 = 1.2 \cdot \delta m^2$, green: $E^2 = 1.4 \cdot \delta m^2$, yellow: $E^2 = 2.3 \cdot \delta m^2$, purple: $E^2 = 3.2 \cdot \delta m^2$; adopting a fixed value of $k = 4/l$). The vacuum mixing angle is fixed to $\cos 2\theta = 0.99$ in both panels. Due to the periodic behaviour of (4.5), the shown survival probability will repeat itself for $x > l$. (Note that the parameters in this plot have been chosen to illustrate the effect. Realistic parameter ranges will be discussed below.)

at the detector do so after having propagated over different travel distances. Note that when the travel distances are larger than the periodic length, periodicity implies that averaging over cosmic sources with $L \gg l$ is equivalent to averaging over l . Therefore we average over the periodic length to get an averaged survival probability

$$\bar{P} = \frac{1}{l} \int_0^l P_{\nu_a \rightarrow \nu_a}(x) dx = \int_0^l \left[\cos^2 \theta \cdot \cos^2 \tilde{\theta}(x) + \sin^2 \theta \cdot \sin^2 \tilde{\theta}(x) \right] dx \quad (4.14)$$

which with the help of (4.5) reduces to

$$\bar{P} = \frac{1}{2} (I \cos 2\theta + 1) \quad (4.15)$$

where

$$I = \frac{1}{l} \int_0^l \frac{\cos 2\theta - \frac{2E^2}{\delta m^2} \left(1 - \frac{1}{\sqrt{1+k^2 x(l-x)}} \right)}{\sqrt{\left(\frac{2E^2}{\delta m^2} \left(1 - \frac{1}{\sqrt{1+k^2 x(l-x)}} \right) - \cos 2\theta \right)^2 + \sin^2(2\theta)}} dx. \quad (4.16)$$

This expression yields an energy dependent transition probability. As can be seen in figure 3, the averaged survival probability breaks down at the resonance energy E_{Res} and is extremely low for higher energies. This corresponds to the fact, that the effect of shortcuts is only relevant at higher energies. For lower energies there is no significant deviation to standard neutrino mixing. Assuming an adiabatic change in the dispersion relation the high and low energy limits for the transition and survival probabilities can be calculated as follows,

$$\bar{P}(E = 0) = \frac{1}{2} (\cos^2 2\theta + 1) \quad (4.17)$$

$$\bar{P}(E \rightarrow \infty) = \frac{1}{2} (1 - \cos(2\theta)). \quad (4.18)$$

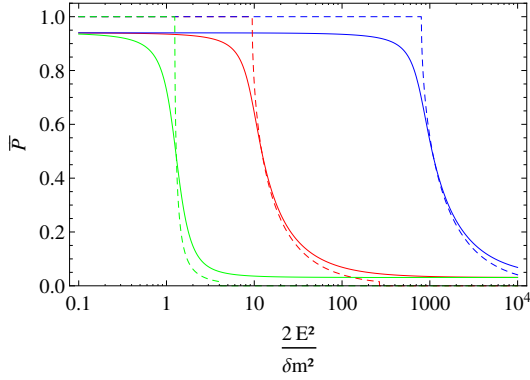


Figure 3. Averaged probability of measuring active neutrino in dependence of the energy-scale $\frac{2E^2}{\delta m^2}$. The different colors correspond to different values of the product kl : Blue: $kl = 0.1$, Red: $kl = 1$, Green: $kl = 10$. The solid lines refer to the light sterile neutrino model with $\sin^2(2\theta) = 0.12$ while the dashed lines refer to the ν MSM-Model with $\sin^2(2\theta) = 10^{-7}$. (Note that the parameters in this plot have been chosen to illustrate the effect. Realistic parameter ranges will be discussed below.)

Model	δm^2	$\sin^2(2\theta)$	E	kl	k^2l/eV	$\frac{\delta m^2 \cos 2\theta}{E^2}$
light sterile neutrino	$(1\text{eV})^2$	0.12	30 TeV	$\gtrsim 10^{-13}$	$\ll 2.2 \cdot 10^{-42}$	10^{-27}
light sterile neutrino	$(1\text{eV})^2$	0.12	1.2 PeV	$\gtrsim 10^{-15}$	$\ll 3.5 \cdot 10^{-47}$	$6.5 \cdot 10^{-31}$
ν MSM	$(1 \text{ keV})^2$	10^{-7}	30 TeV	$\gtrsim 10^{-11}$	$\ll 5.5 \cdot 10^{-29}$	$1.1 \cdot 10^{-21}$
ν MSM	$(1 \text{ keV})^2$	10^{-7}	1.2 PeV	$\gtrsim 10^{-13}$	$\ll 3.5 \cdot 10^{-32}$	$6.9 \cdot 10^{-25}$

Table 2. Regions in the parameter space of k and l where resonant conversion occurs in various parameter sets and neutrino energies E .

The survival probability \bar{P} depends only on the product of the geometric parameters k and l . As can be seen the fall-off of the survival probability is shifted to higher energies for smaller factors kl . This corresponds to a smaller ratio of the initial velocities $\frac{|u_0|}{x_0}$. For smaller kl the sterile neutrino thus plunges less deeply into the bulk and thus is less affected by the shortcut, therefore it needs a have higher energy to experience resonant conversion.

Fixing the product kl and varying the vacuum mixing angle does not affect the position of the tilt in the conversion probability but makes the function steeper for smaller vacuum mixing angles.

For a given set of mixing parameters δm^2 , $\sin^2(2\theta)$ and a given energy E we obtain the following constraints for the geometric parameters k and l :

If the product kl is too small, no level crossing will occur in the non adiabatic region, and consequently no resonant conversion will emerge. On the other hand, if the product k^2l is too large, the adiabatic condition will not be fulfilled and the level crossing will not result in resonant conversion. Additionally for large periodic length l there is a lower bound for the product k^2l which ensures that the resonance length is much smaller than the expected travel distance. Adopting again the parameter sets for light sterile and ν MSM neutrinos discussed above, and requiring a transition probability $> 75 \%$ we arrive at the conditions under which the major part of ν_2 and ν_3 and therefore a large part of muon and tau neutrinos are converted into sterile neutrinos. Numerical values for various parameter sets and neutrino energies are given in table 2.

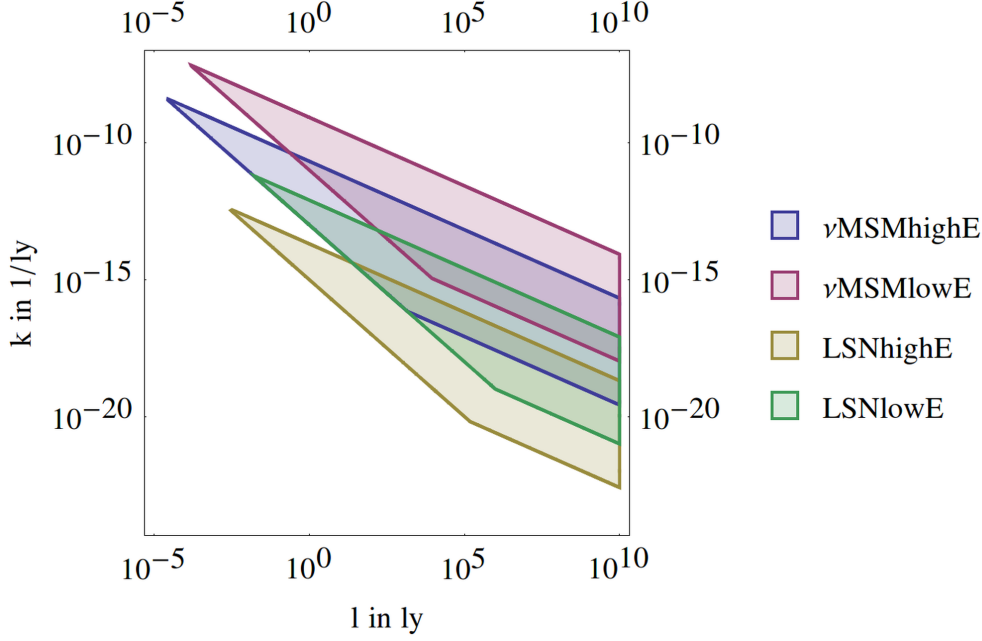


Figure 4. Regions in the parameter space of k and l where resonant conversion occurs. Bounds on the resonance length from atmospheric/solar neutrino oscillations have been taken into account. The different cases depicted correspond to a ν MSM neutrino and a light sterile neutrino (LSN) with energies of 30 TeV and 1.2 PeV.

Figure 4 displays the bounds obtained on k and l . As can be seen the periodic length l has to be very large to fulfill both conditions. Additionally figure 5 shows the allowed regions for the geometric parameters when the whole energy region from 30 TeV up to 1.2 PeV should be affected. Also taken into account is the constraint resulting from the fact that atmospheric and solar neutrino data are in conflict with significant oscillation or conversion into sterile neutrinos. In order to have atmospheric and solar neutrinos unaffected by the change in the dispersion relation we assume that the resonance length is much larger than the distance from the Earth to the sun

$$x_{res} > 8 \cdot 10^{17} \frac{1}{\text{eV}} = 1.6 \cdot 10^{-5} \text{ly} \quad (4.19)$$

which leads to

$$k^2 l < \frac{1}{8} 10^{-17} \text{eV} \frac{\delta m^2 \cos 2\theta}{2E^2}. \quad (4.20)$$

As can be seen in figures 4 and 5 large parts of the parameter space are consistent with all constraints and allow for a significant reduction of the rates of astrophysical muon and tau neutrinos.

5 Conclusion

In summary, we have discussed the effect of altered dispersion relations for sterile neutrinos propagating in extra dimensions on the flavor ratios of astrophysical neutrinos. We have confined our discussion to two important limits: the case where the extra-dimensional shortcut can be described in terms of a constant effective potential and the case where the potential

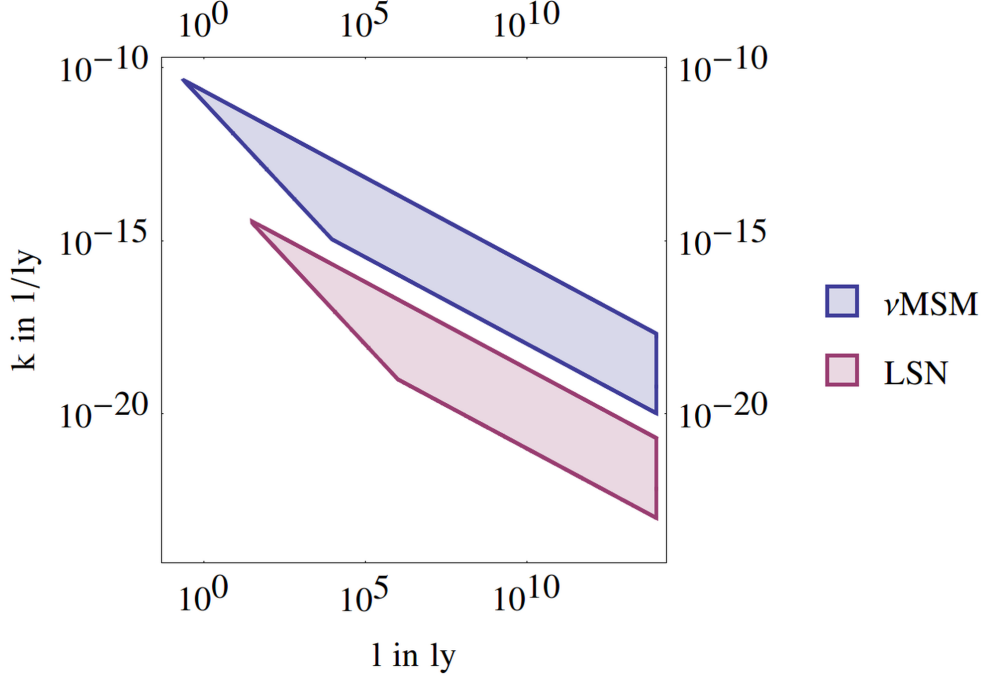


Figure 5. As Fig. 4, but displaying the regions in parameter space where resonant conversion occurs in the entire interval from 30 TeV to 1.2 PeV.

changes adiabatically giving rise to an MSW-like resonant flavor conversion. In the first case one gets significant distortions of the expected flavor ratio around the resonance region whose width depends strongly on the active-sterile neutrino mixing. In the second case strong deviations, including a significant suppression of muon and tau neutrino fluxes are possible over a large range of energies and baselines. This effect arises only for energies above the resonance energy and may be a possible explanation for the unexpected energy dependence reported in [8]. The flavor ratios of high energy astrophysical neutrinos thus qualify as a prime probe for non-standard dispersion relations originating from exotic physics such as shortcuts in extra dimensions.

Acknowledgments

We thank Danny Marfatia and our first referee for useful discussions. HP was supported by the 'Helmholtz Alliance for Astroparticle Physics HAP' funded by the Initiative and Networking Fund of the Helmholtz Association. SP was supported by the US DOE grant DE-Fc02-04ER41201 and the Alexander von Humboldt Foundation and acknowledges TU Dortmund for kind hospitality. HP and SP thank the KITP Santa Barbara for kind hospitality. This research was supported in part by the National Science Foundation under Grant No. NSF PHY11-25915.

References

- [1] M. G. Aartsen *et al.* [IceCube Collaboration], Phys. Rev. Lett. **113** (2014) 101101 [arXiv:1405.5303 [astro-ph.HE]].

- [2] M. G. Aartsen *et al.* [IceCube Collaboration], “Evidence for High-Energy Extraterrestrial Neutrinos at the IceCube Detector,” *Science* **342** (2013) 1242856 [arXiv:1311.5238 [astro-ph.HE]].
- [3] S. Pakvasa, A. Joshipura and S. Mohanty, “Explanation for the low flux of high energy astrophysical muon-neutrinos,” *Phys. Rev. Lett.* **110** (2013) 171802 [arXiv:1209.5630 [hep-ph]].
- [4] L. Dorame, O. G. Miranda and J. W. F. Valle, “Invisible decays of ultra-high energy neutrinos,” arXiv:1303.4891 [hep-ph].
- [5] O. Mena, S. Palomares-Ruiz and A. C. Vincent, “On the flavor composition of the high-energy neutrino events in IceCube,” *Phys. Rev. Lett.* **113** (2014) 091103 [arXiv:1404.0017 [astro-ph.HE]].
- [6] C. Y. Chen, P. S. B. Dev and A. Soni, “Standard Model Explanation of the Ultra-high Energy Neutrino Events at IceCube,” *Phys. Rev. D* **89** (2014) 033012 [arXiv:1309.1764 [hep-ph]].
- [7] L. A. Anchordoqui, V. Barger, I. Cholis, H. Goldberg, D. Hooper, A. Kusenko, J. G. Learned and D. Marfatia *et al.*, “Cosmic Neutrino Pevatrons: A Brand New Pathway to Astronomy, Astrophysics, and Particle Physics,” *Journal of High Energy Astrophysics* **1-2** (2014) 1 [arXiv:1312.6587 [astro-ph.HE]].
- [8] S. Palomares-Ruiz, A. C. Vincent and O. Mena, “Spectral analysis of the high-energy IceCube neutrinos,” arXiv:1502.02649 [astro-ph.HE].
- [9] A. Palladino, G. Pagliaroli, F. L. Villante and F. Vissani, “Which is the flavor of cosmic neutrinos seen by IceCube?,” arXiv:1502.02923 [astro-ph.HE].
- [10] M. G. Aartsen *et al.* [IceCube Collaboration], “Flavor Ratio of Astrophysical Neutrinos above 35 TeV in IceCube,” arXiv:1502.03376 [astro-ph.HE].
- [11] H. Päs, S. Pakvasa and T. J. Weiler, “Sterile-active neutrino oscillations and shortcuts in the extra dimension,” *Phys. Rev. D* **72** (2005) 095017 [hep-ph/0504096].
- [12] D. J. H. Chung and K. Freese, “Can geodesics in extra dimensions solve the cosmological horizon problem?,” *Phys. Rev. D* **62** (2000) 063513 [hep-ph/9910235].
- [13] D. J. H. Chung and K. Freese, “Cosmological challenges in theories with extra dimensions and remarks on the horizon problem,” *Phys. Rev. D* **61** (2000) 023511 [hep-ph/9906542].
- [14] C. Csaki, J. Erlich and C. Grojean, “Gravitational Lorentz violations and adjustment of the cosmological constant in asymmetrically warped space-times,” *Nucl. Phys. B* **604** (2001) 312 [hep-th/0012143].
- [15] S. Hollenberg, O. Micu, H. Päs and T. J. Weiler, “Baseline-dependent neutrino oscillations with extra-dimensional shortcuts,” *Phys. Rev. D* **80** (2009) 093005 [arXiv:0906.0150 [hep-ph]].
- [16] J. Kopp, P. A. N. Machado, M. Maltoni and T. Schwetz, “Sterile Neutrino Oscillations: The Global Picture,” *JHEP* **1305**, 050 (2013) [arXiv:1303.3011 [hep-ph]].
- [17] H. Päs, S. Pakvasa, J. Dent and T. J. Weiler, “Closed timelike curves in asymmetrically warped brane universes,” *Phys. Rev. D* **80** (2009) 044008 [gr-qc/0603045].
- [18] J. Dent, H. Päs, S. Pakvasa and T. J. Weiler, “Neutrino time travel,” In **Karlsruhe 2007, SUSY 2007** 760-763 [arXiv:0710.2524 [hep-ph]].
- [19] S. Hollenberg and H. Päs, “Resonant active-sterile neutrino mixing in the presence of matter potentials and altered dispersion relations,” arXiv:0904.2167 [hep-ph].
- [20] D. Marfatia, H. Päs, S. Pakvasa and T. J. Weiler, “A model of superluminal neutrinos,” *Phys. Lett. B* **707** (2012) 553 [arXiv:1112.0527 [hep-ph]].
- [21] O. G. Miranda, C. A. Moura and A. Parada, “Sterile neutrinos, dark matter, and resonant effects in ultra high energy regimes,” arXiv:1308.1408 [hep-ph].

- [22] J. F. Beacom, N. F. Bell, D. Hooper, S. Pakvasa and T. J. Weiler, “Measuring flavor ratios of high-energy astrophysical neutrinos,” *Phys. Rev. D* **68**, 093005 (2003) [Erratum-ibid. *D* **72**, 019901 (2005)] [hep-ph/0307025].
- [23] K. -C. Lai, G. -L. Lin and T. C. Liu, “Determination of the Neutrino Flavor Ratio at the Astrophysical Source,” *Phys. Rev. D* **80**, 103005 (2009) [arXiv:0905.4003 [hep-ph]].
- [24] S. Pakvasa, W. Rodejohann and T. J. Weiler, “Flavor Ratios of Astrophysical Neutrinos: Implications for Precision Measurements,” *JHEP* **0802**, 005 (2008) [arXiv:0711.4517 [hep-ph]].
- [25] P. F. Harrison, D. H. Perkins and W. G. Scott, “Tri-bimaximal mixing and the neutrino oscillation data,” *Phys. Lett. B* **530** (2002) 167 [hep-ph/0202074].
- [26] L. S. Kisslinger, “Sterile Plus Active Neutrinos and Neutrino Oscillations,” arXiv:1309.4983 [hep-ph].
- [27] J. G. Learned and S. Pakvasa, “Detecting tau-neutrino oscillations at PeV energies,” *Astropart. Phys.* **3** (1995) 267 [hep-ph/9405296, hep-ph/9408296].
- [28] H. Athar, M. Jezabek and O. Yasuda, “Effects of neutrino mixing on high-energy cosmic neutrino flux,” *Phys. Rev. D* **62** (2000) 103007 [hep-ph/0005104].
- [29] D. V. Ahluwalia, C. A. Ortiz, G. Z. Adunas and , “Robust flavor equalization of cosmic neutrino flux by quasi bimaximal mixing,” hep-ph/0006092.
- [30] T. Asaka, M. Laine and M. Shaposhnikov, “Lightest sterile neutrino abundance within the nuMSM,” *JHEP* **0701** (2007) 091 [hep-ph/0612182].
- [31] J. F. Beacom, N. F. Bell, D. Hooper, S. Pakvasa and T. J. Weiler, “Sensitivity to θ_{13} and δ in the decaying astrophysical neutrino scenario,” *Phys. Rev. D* **69** (2004) 017303 [hep-ph/0309267].
- [32] L. Wolfenstein, “Neutrino Oscillations in Matter,” *Phys. Rev. D* **17** (1978) 2369.
- [33] V. D. Barger, K. Whisnant, S. Pakvasa and R. J. N. Phillips, “Matter Effects on Three-Neutrino Oscillations,” *Phys. Rev. D* **22** (1980) 2718.
- [34] S. P. Mikheev and A. Y. Smirnov, “Resonant amplification of neutrino oscillations in matter and solar neutrino spectroscopy,” *Nuovo Cim. C* **9** (1986) 17.
- [35] H. Päs, P. Sicking, M. Supsar, “ Neutrino oscillations in asymmetrically warped space times”, to be published